Core dynamo simulations of A-type stars

J.P. Hidalgo[1], P.J. Käpylä[2], C.A. Ortiz-Rodríguez[3], F.H. Navarrete[4], D.R.G. Schleicher[1] & B. Toro-Velásquez[1]

[1] *Departamento de Astronomía, Universidad de Concepción, Chile*
[2] *Institut für Sonnenphysik, KIS, Alemania*
[3] *Hamburger Sternwarte, Universität Hamburg, Alemania*
[4] *Institute of Space Sciences, ICE–CSIC, España*

Received: 09 February 2024 / Accepted: 29 March 2024

Resumen / Las estrellas tipo A tienen núcleos convectivos y envoltorios radiativos. Realizamos simulaciones numéricas en 3D de una estrella tipo A de 2 $M_\odot$ con un núcleo convectivo de aproximadamente 20 % del radio estelar rodeado por una envoltura radiativa usando un modelo star-in-a-box, como una forma de explorar campos magnéticos impulsados por la convección en el núcleo de la estrella. Las ecuaciones no ideales totalmente compresibles de la magnetohidrodinámica son resueltas ocupando el Pencil Code. Periodos de rotación desde 8 a 20 días fueron explorados. Concluimos que el núcleo es capaz de albergar fuertes dínamos hemisféricos con comportamiento cíclico y campos magnéticos con intensidades típicas alrededor de los 60 kG. Sin embargo, los campos magnéticos que llegan a la superficie son varios órdenes de magnitud menores que en el núcleo, lo que no es suficiente para explicar los campos magnéticos observados.

Abstract / A-type stars have convective cores and radiative envelopes. We perform 3D numerical simulations of a 2 $M_\odot$ A-type star with a convective core of roughly 20% of the stellar radius surrounded by a radiative envelope using a star-in-a-box model, as a way to explore magnetic fields driven by convection in the core of the star. The non-ideal fully compressible magnetohydrodynamics equations were solved using the Pencil Code. Rotation periods from 8 to 20 days were explored. We conclude that the core is able to host strong hemispheric dynamos with cyclic behavior and typical magnetic field strengths around 60 kG. However, the magnetic fields that reach the surface are several orders of magnitude smaller than in the core, which is not enough to explain the observed magnetic fields.

Keywords / stars: magnetic field — stars: massive — magnetohydrodynamics (MHD) — dynamo

1. Introduction

Early-type stars are main-sequence stars with masses above 1.5 $M_\odot$. In these stars, the main energy production mechanism is the CNO cycle. This cycle is very temperature dependent, and therefore a large energy flux is concentrated in the center of the star leading to a steep temperature gradient that drives convection. The convective cores of these stars have differential rotation and regions of shear that are favorable for dynamo action (Krause & Oetken, 1976; Browning, 2008). Numerical simulations by Brun et al. (2005) showed a core dynamo in a 2 $M_\odot$ A-type star, modelling the inner 30% by radius where 15% is the core. The magnetic energy produced in their models is around equipartition with kinetic energy. In B-type stars dynamo action has been found as well. Simulations by Augustson et al. (2016) of the inner 65% by radius of a 10 $M_\odot$ B-type star show vigorous dynamo action. The resulting magnetic fields have peaks exceeding a megagauss and reach superequipartition values. Nevertheless, despite these studies reporting that a convective core can lead to strong dynamo action, the nature of these dynamos has not been explored in detail. The produced magnetic fields could play an important role in the observed magnetism of Ap/Bp stars. These stars are a chemically peculiar subclass of early-type stars with masses ranging from 1.5 to 6 $M_\odot$, and large-scale magnetic fields with mean field strengths ranging from 200 G to 30 kG Aurière et al. (2007).

In the present study, we perform 3D magnetohydrodynamic (MHD) simulations of a main-sequence A-type star using a star-in-a-box setup and model the entire star for the first time in 3D numerical simulations. Our main objective is to study and characterize the core dynamos of such stars, and to analyze the resulting magnetic fields at the stellar surface. Differential rotation is also explored, at the surface of the convective core and at the stellar surface. The structure of this paper is the following: The model is described in Section 2. The analysis and results of the simulations are presented in Section 3. Conclusions are provided in Section 4.

2. The Model

The model is based on the star-in-a-box setup presented by Käpylä (2021), which is based on the model of Dobler et al. (2006). The setup consists in a star of radius R

✉ *Contact* / jhidalgo2018@udec.cl

inside a cube of side $l = 2.2R$. All the Cartesian coordinates (x, y, z) range from $-l/2$ to $l/2$. The following non-ideal fully compressible MHD equation set is solved:

$$\frac{\partial \boldsymbol{A}}{\partial t} = \boldsymbol{u} \times \boldsymbol{B} - \eta\mu_0 \boldsymbol{J}, \tag{1}$$

$$\frac{D \ln \rho}{Dt} = -\boldsymbol{\nabla} \cdot \boldsymbol{u}, \tag{2}$$

$$\frac{D\boldsymbol{u}}{Dt} = -\boldsymbol{\nabla}\Phi - \frac{1}{\rho}\left(\boldsymbol{\nabla} p - \boldsymbol{\nabla} \cdot 2\nu\rho\boldsymbol{S} + \boldsymbol{J} \times \boldsymbol{B}\right) - 2\boldsymbol{\Omega} \times \boldsymbol{u} + \boldsymbol{f}_d, \tag{3}$$

$$T\frac{Ds}{Dt} = -\frac{1}{\rho}\left[\boldsymbol{\nabla} \cdot (\boldsymbol{F}_{\rm rad} + \boldsymbol{F}_{\rm SGS}) + \mathcal{H} - \mathcal{C} + \mu_0\eta\boldsymbol{J}^2\right] + 2\nu\boldsymbol{S}^2, \tag{4}$$

where $\boldsymbol{A}$ is the magnetic vector potential, $\boldsymbol{u}$ is the flow velocity, $\boldsymbol{B} = \boldsymbol{\nabla} \times \boldsymbol{A}$ is the magnetic field, η is the magnetic diffusivity, μ_0 is the magnetic permeability of vacuum, $\boldsymbol{J} = \boldsymbol{\nabla} \times \boldsymbol{B}/\mu_0$ is the current density given by Ampère's law, $D/Dt = \partial/\partial t + \boldsymbol{u} \cdot \boldsymbol{\nabla}$ is the advective derivative, ρ is the mass density, Φ is the gravitational potential, p is the pressure, ν is the kinematic viscosity, $\boldsymbol{S}$ is the traceless rate-of-strain tensor

$$S_{ij} = \frac{1}{2}(\partial_j u_i + \partial_i u_j) - \frac{1}{3}\delta_{ij}\boldsymbol{\nabla} \cdot \boldsymbol{u}, \tag{5}$$

where δ_{ij} is the Kronecker delta. $\boldsymbol{\Omega} = (0, 0, \Omega_0)$ is the rotation vector, $\boldsymbol{f}_{\rm d}$ describes damping of flows outside the star (see Dobler et al., 2006, for details), T is the temperature, and s is the specific entropy. The radiative energy flux is given by

$$\boldsymbol{F}_{\rm rad} = -K\boldsymbol{\nabla}T, \tag{6}$$

where K is the constant radiative heat conductivity. Additionally, the subgrid-scale (SGS) entropy flux is defined as

$$\boldsymbol{F}_{\rm SGS} = -\chi_{\rm SGS}\rho\boldsymbol{\nabla}s', \tag{7}$$

where $\chi_{\rm SGS}$ is the SGS diffusion coefficient, and s' is the fluctuating entropy. Finally, $\mathcal{H}$ and $\mathcal{C}$ describe additional heating and cooling, respectively. For these we adopt similar expressions as in Käpylä (2021). The ideal gas equation of state $p = (\gamma - 1)\rho e$ is assumed, where γ is the adiabatic index and e is the internal energy of the gas. We use radial profiles for the diffusivities ν and η, where the radiative layers have values 10^2 times smaller than in the core. We define the radial jumps at $r = 0.35R$ with a width of $w = 0.06R$. This implementation aims to avoid the spreading of magnetic fields and flows from the core to the envelope (see Käpylä, 2022).

The model has a convective core of roughly 20% of the stellar radial extent surrounded by a radiative envelope. The heat conductivity coefficient $K = 0.1K_0$ leads to such configuration in the thermally relaxed state, where K_0 is the value required for a fully radiative configuration (see Fig. 1 of Hidalgo et al. 2023). The stellar parameters for a 2 $M_\odot$ A-type star are $R_* = 2\ R_\odot$, $\rho_0 = 5.6 \cdot 10^4$ kg m^{-3}, $T_0 = 2.25 \cdot 10^7$ K and $L_* = 23\ L_\odot$ for the radius, mass density and temperature of the stellar center, and luminosity, respectively. These parameters are obtained from a one dimensional stellar model from the open-source code MESA (Paxton et al., 2019). For the conversion to physical units, the description in the Appendix A of Käpylä et al. (2020) is followed. The simulations were run on a grid of 200^3 with the Pencil Code* (Pencil Code Collaboration et al., 2021), which is a highly modular high-order finite-difference code for solving ordinary and partial differential equations.

Table 1. Summary of the simulations. From left to right the columns correspond to the rotation period $P_{\rm rot} = 2\pi/\Omega_0$ in [days], the volume averaged (over the convective zone) root-mean-square flow velocity $u_{\rm rms}$ in [m s^{-1}], the volume-averaged root-mean-square magnetic field $B_{\rm rms}$ in [kG], the Coriolis number, and the fluid and magnetic Reynolds numbers.

Run	$P_{\rm rot}$	$u_{\rm rms}$	$B_{\rm rms}$	Co	Re	$\mathrm{Re_M}$
MHDr1	20	98	no dynamo	4.9	54	38
MHDr2	15	50	59	10.1	35	24
MHDr3	10	38	64	19.2	27	19
MHDr4	8	35	59	26.9	24	17

2.1. Dimensionless parameters

To characterize each simulation the following dimensionless parameters are computed. The influence of rotation on the flow is measured by the Coriolis number

$$\mathrm{Co} = \frac{2\Omega_0}{u_{\rm rms}k_R}, \tag{8}$$

where $u_{\rm rms}$ is the root-mean-square velocity averaged over the convective zone ($r < 0.2R$) and $k_R = 2\pi/0.2R$ is the wave number of the largest convective eddies. The fluid and magnetic Reynolds numbers are

$$\mathrm{Re} = \frac{u_{\rm rms}}{\nu k_R}, \qquad \mathrm{Re_M} = \frac{u_{\rm rms}}{\eta k_R}. \tag{9}$$

The magnetic and SGS Prandtl numbers are

$$\mathrm{Pr_M} = \frac{\nu}{\eta}, \qquad \mathrm{Pr_{SGS}} = \frac{\nu}{\chi_{\rm SGS}}.$$

3. Results

We present a set of simulations exploring rotation periods from 8 to 20 days. All of the runs have diffusivities $\nu = 5.45 \cdot 10^7$ [m^2/s], $\eta = 7.78 \cdot 10^7$ [m^2/s], and $\chi_{\rm SGS} = 2.61 \cdot 10^8$ [m^2/s] in the core. Therefore $\mathrm{Pr_M} \approx 0.7$ and $\mathrm{Pr_{SGS}} \approx 0.21$. The simulations, as well as the diagnostic quantities are listed in Table 1.

The density stratification between the center and the surface of the convective core is $\rho_{\rm center}/\rho_{\rm surfcore} \approx 1.27$, which is close to the MESA model result $\rho_{\rm center}/\rho_{\rm surfcore} \approx 1.5$. Furthermore, the ratio between the temperature of the center and the surface of the convective core is $T_{\rm center}/T_{\rm surfcore} \approx 1.25$.

*https://pencil-code.org/

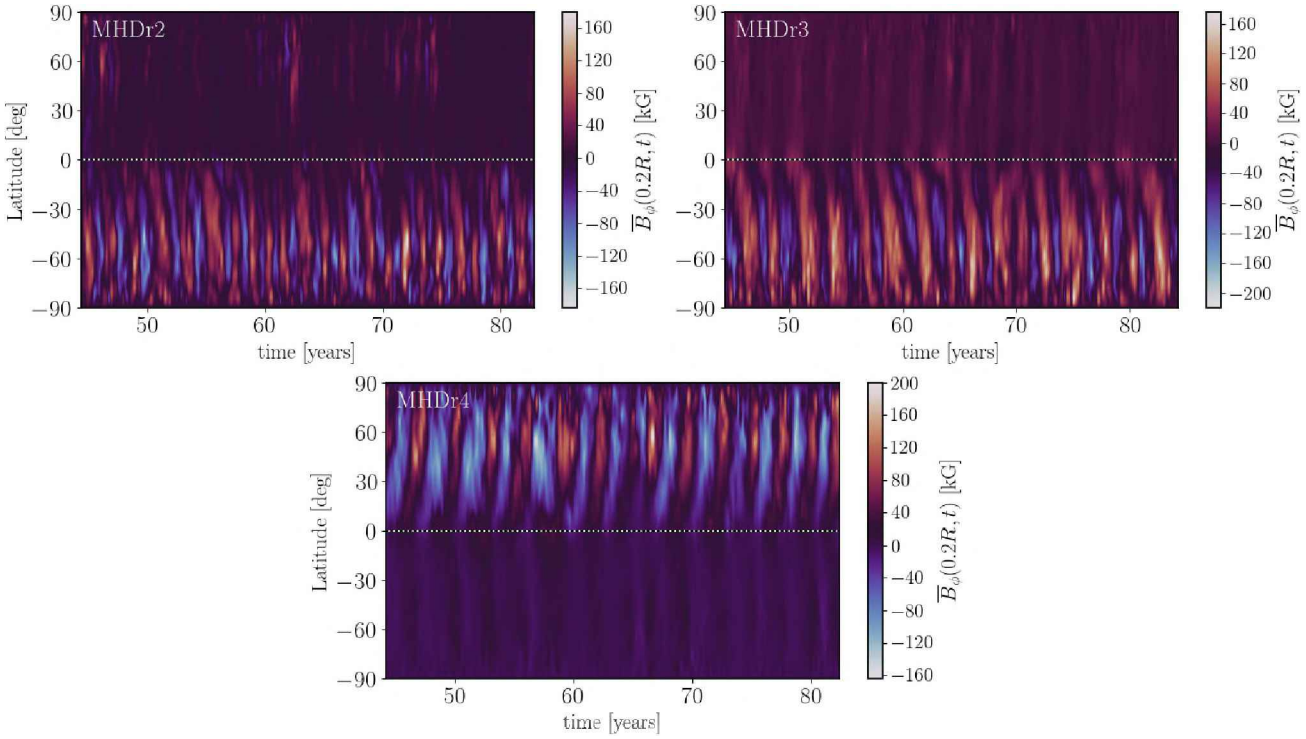

Fig. 1. Time-latitude diagrams of the azimuthally averaged toroidal magnetic field $\overline{B}_\phi(r = 0.2R, \theta, t)$. The run is indicated in the upper left corner of each plot.

3.1. Core dynamos

Run MHDr1 does not have a dynamo. All the remaining runs have core dynamos. The azimuthally averaged toroidal magnetic fields $\overline{B}_\phi(r, \theta, t)$ at $r = 0.2R$ are shown in Fig. 1. All of the solutions are hemispheric and cyclic. In Runs MHDr2 and MHDr3 the magnetic field is located in the southern hemisphere, while in MHDr4 the magnetic activity is located in the northern hemisphere. Cyclic solutions have been reported in simulations of fully convective stars (see e.g. Käpylä, 2021; Ortiz-Rodríguez et al., 2023). However, these solutions are usually in both hemispheres of the star. A notable exception are the spherical simulations of fully convective M dwarfs by Brown et al. (2020). In these runs the obtained global-scale mean magnetic fields are hemispheric (see their Fig. 1). The reason behind these hemispheric solutions is currently unclear.

The total kinetic and magnetic energies are

$$E_{\rm kin} = \frac{1}{2}\int_{V_*} \rho \boldsymbol{u}^2 dV, \tag{10}$$

$$E_{\rm mag} = \frac{1}{2\mu_0}\int_{V_*} \boldsymbol{B}^2 dV, \tag{11}$$

where V_* is the volume of the star. The runs have magnetic energies below equipartition. However, as rotation increases, the ratio $E_{\rm mag}/E_{\rm kin}$ increases, reaching a nearly equipartition regime similar to that reported by Brun et al. (2005) in the core. This behavior is visible in Fig. 2, where the total energies are shown according to equations (10) and (11). All our simulations have magnetic fields with roughly the same mean strength of $B_{\rm rms} \approx 60$ kG, see Table 1.

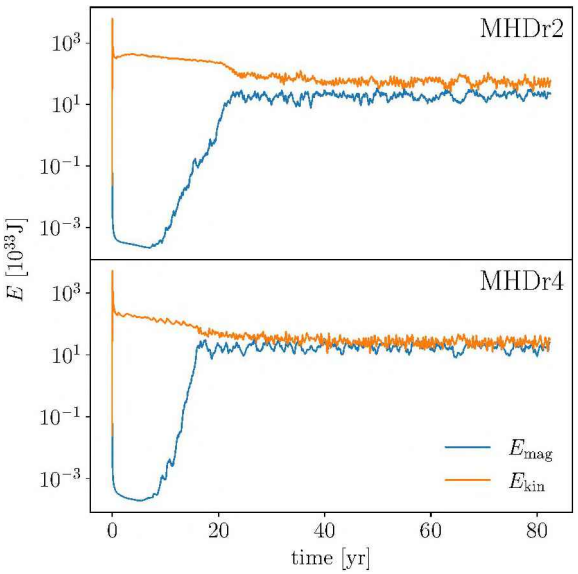

Fig. 2. Temporal evolution of the magnetic and kinetic energies from runs MHDr2 (*top panel*) and MHDr4 (*bottom panel*).

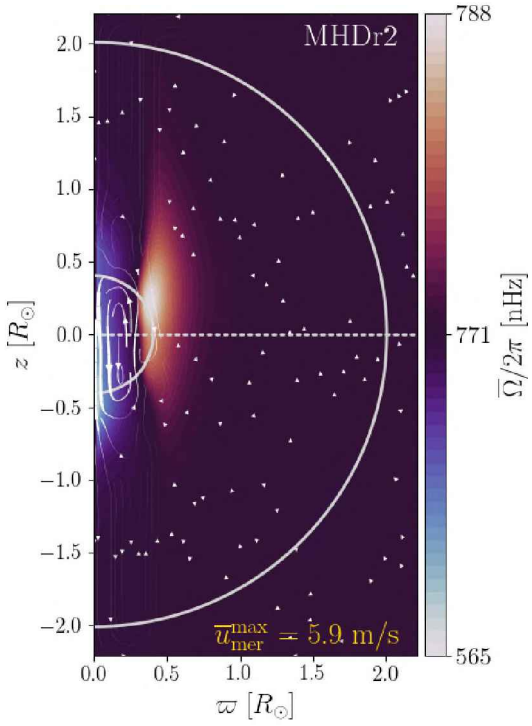

Fig. 3. Profile of the temporally and azimuthally averaged rotation rate $\overline{\Omega}(\varpi, z)$ of MHDr2. The streamlines indicate the mass flux due to meridional circulation and the maximum averaged meridional flow is indicated in the lower left side of the plot. The dashed line represents the equator.

3.2. Differential rotation

The azimuthally averaged rotation rate is

$$\overline{\Omega}(\varpi, z) = \Omega_0 + \overline{u}_\phi(\varpi, z)/\varpi, \tag{12}$$

where $\varpi = r \sin\theta$ is the cylindrical radius. Furthermore, the average meridional flow is

$$\overline{\boldsymbol{u}}_{\rm mer} = (\overline{u}_\varpi, 0, \overline{u}_z). \tag{13}$$

The rotation profile $\overline{\Omega}(\varpi, z)$ of MHDr2 is shown in Fig. 3. The core has solar-like differential rotation, i.e., the equator rotates faster than the poles. Moreover, the stellar surface and a substantial part of the radiative envelope have quasi-rigid rotation. The rotation profile is asymmetric with respect to the equator. This is a consequence of the hemispheric dynamo, which quenches the differential rotation in its corresponding hemisphere. The rest of simulations have very similar rotation profiles.

3.3. Surface magnetic fields

The magnetic fields produced by the core dynamo are unable to create large-scale structures in the stellar surface. The root-mean-square of $\overline{B}_\phi(r, \theta, \phi)$ in latitudes from -90 to -75 and 75 to 90 degrees has values around 0.1 kG, while in the rest of latitudes it has the order of 10^{-5} kG. Therefore, the magnetic field is nearly zero on almost the whole surface of the star, except at the poles.

4. Conclusions

We perform star-in-a-box simulations of a 2 $M_\odot$ A-type star, where the convective core corresponds to 20% of the radial extent. Rotation rates from 8 to 20 days are explored. We find core dynamos with magnetic fields with typical strengths around 60 kG. All the dynamo solutions are hemispheric and cyclic, similar to the results reported by Brown et al. (2020). In the fast rotators the magnetic energy is nearly in equipartition with the kinetic energy. Unlike Augustson et al. (2016), none of our runs reached super-equipartition values. The simulations exhibit solar-like differential rotation in the core, and quasi-rigid rotation in a large part of the radiative envelope. We conclude that a core dynamo is not enough to explain the observed magnetism of Ap/Bp stars, and different mechanisms should be explored. A natural next step is to add a fossil field in our model, as it can affect the nature of the core dynamo (Featherstone et al., 2009). Finally, the cycles of the dynamo solutions require further analysis, e.g. a magnetic cycle period $P_{\rm cyc}$ can be computed. This would allow to study possible relations between the magnetic cycle period and rotation (see e.g. Warnecke, 2018; Käpylä, 2022).

Acknowledgements: JPH and DRGS gratefully acknowledge support by the ANID BASAL projects ACE210002 and FB21003, as well as via Fondecyt Regular (project code 1201280). The simulations were performed with resources provided by the Kultrun Astronomy Hybrid Cluster via the projects Conicyt Quimal #170001, Conicyt PIA ACT172033, and Fondecyt Iniciacion 11170268. PJK was supported in part by the Deutsche Forschungsgemeinschaft (DFG, German Research Foundation) Heisenberg programme (grant No. KA 4825/4-1), and by the Munich Institute for Astro-, Particle and BioPhysics (MIAPbP) which is funded by the DFG under Germany's Excellence Strategy – EXC-2094 – 390783311.

References

Augustson K.C., Brun A.S., Toomre J., 2016, ApJ, 829, 92
Aurière M., et al., 2007, A&A, 475, 1053
Brown B.P., et al., 2020, ApJL, 902, L3
Browning M.K., 2008, ApJ, 676, 1262
Brun A.S., Browning M.K., Toomre J., 2005, ApJ, 629, 461
Dobler W., Stix M., Brandenburg A., 2006, ApJ, 638, 336
Featherstone N.A., et al., 2009, ApJ, 705, 1000
Hidalgo J.P., et al., 2023, Boletin de la Asociacion Argentina de Astronomia La Plata Argentina, 64, 50
Käpylä P.J., 2021, A&A, 651, A66
Käpylä P.J., 2022, ApJL, 931, L17
Käpylä P.J., et al., 2020, Geophysical and Astrophysical Fluid Dynamics, 114, 8
Krause F., Oetken L., 1976, W.W. Weiss, H. Jenkner, H.J. Wood (Eds.), *IAU Colloq. 32: Physics of Ap Stars*, 29
Ortiz-Rodríguez C.A., et al., 2023, A&A, 678, A82
Paxton B., et al., 2019, ApJS, 243, 10
Pencil Code Collaboration, et al., 2021, The Journal of Open Source Software, 6, 2807
Warnecke J., 2018, A&A, 616, A72